ANALES de Edificación

Anales de Edificación Vol. 4,
Nº 3, 52-58 (2018)
ISSN: 2444-1309
Doi: 10.20868/ade.2018.3800

Received: 06-08-2018
Accepted:20-08-2018

Parámetros de la Fractura del Hormigón Reforzado con Fibras de Basalto.
Fracture Parameters of Basalt Fiber Reinforced Concrete.

Marta Kosior-Kazberuk[a], Julita Krassowska[a], Alejandra Vidales Barriguete[b] & Carolina Piña Ramirez[b]

[a]Faculty of Civil and Environmental Engineering, Bialystok University of Technology, (Poland, m.kosior@pb.edu.pl, j.krassowska@pb.edu.pl), [b]Departamento de Tecnología de la Edificación, Escuela Técnica Superior de Edificación, UPM, Madrid (Spain, alejandra.vidales@upm.es, carolina.pina@upm.es)

Resumen— **En el estudio se utilizó un método de flexión de tres puntos para determinar la tenacidad de la fractura de los hormigones con fibras de basalto. Las propiedades de fractura y el comportamiento posterior al agrietamiento del hormigón, se analizaron sobre la base de las curvas de desplazamiento de la abertura de grietas de carga (*P*-CMOD). Las fibras de basalto cortadas (50 mm de longitud, 0,02 mm de diámetro) se agregaron al hormigón de cemento con un contenido de 2,0; 4,0 y 8,0 kg/m^3. La adición de la fracción volumétrica considerada de fibras de basalto tuvo una influencia significativa en las propiedades de fractura del hormigón, mientras que las fibras tuvieron un ligero efecto en las propiedades de resistencia del hormigón. Las fibras de basalto causaron la mejora de los parámetros de fractura como K_{Ic}, $CTOD_c$ y la energía de fractura total G_F. El análisis de los diagramas *P*-CMOD demostró que el comportamiento de la fractura después de la fractura del haz se mejoró mucho mediante la adición de fibras de basalto. Los resultados de la medición de la dureza y las características de absorción de energía mostraron que las muestras de hormigón reforzado con fibrasmejoran su comportamiento dúctil y su capacidad de absorción de energía, en comparación con las muestras de hormigón ordinario.**

Palabras clave: Hormigón, Fibras de basalto, Fractura mecánica, Comportamiento posterior al agrietamiento.

Abstract— **A three-point bending method was used in the study to determine the fracture toughness of concretes with basalt fibers. The post-cracking behavior and fracture properties of concrete were analyzed on the basis of load–crack mouth opening displacement (*P*–CMOD) curves. The chopped basalt fibers (50 mm length; 0.02 mm diameter) were added to cement concrete at the contents of 2,0; 4,0 and 8,0 kg/m^3. The addition of the considered volume fraction of basalt fibers had significant influence on the fracture properties of concrete, while the fibers had slight effect on the strength properties of concrete. The basalt fibers caused the improvement of the fracture parameters as K_{Ic}, $CTOD_c$ and total fracture energy G_F. The analysis of *P*-CMOD diagrams proved that the post-cracking fracture behavior of the beam was greatly improved by the addition of basalt fibers. The results of measuring the toughness and energy-absorption characteristics showed that fiber reinforced concrete specimens acquire a great ductile behavior and energy absorption capacity, compared to ordinary concrete specimens.**

Index Terms: Concrete, Basalt fiber, Fracture mechanics, Post-cracking behavior.

M. Kosior-Kazberuk and Julita Krassowska are from the Department of Building Structures and Architecture, Faculty of Civil and Environmental Engineering, Bialystok University of Technology, Poland (e-mail: m.kosior@pb.edu.pl, j.krassowska@pb.edu.pl).

A.Vidales Barriguete and C. Piña Ramirez are members of Departamento de Tecnología de la Edificación, Escuela Técnica Superior de Edificación, Universidad Politechnic de Madrid, Madrid, Spain (e-mail: alejandra.vidales@upm.es, carolina.pina@upm.es).

I. Introduction

The use of non-metallic reinforcement in civil engineering is increasingly common (High et al., 2015). The main purpose of the fibers is to provide a control of cracking and to increase the fracture toughness of the brittle cement matrix through bridging action during both micro and macrocracking of the matrix. The ductility characteristic is dependent on the fiber type and dosage, tensile strength and anchorage mechanism. In recent years, chopped basalt fibers (BFs) have gained popularity among others due to their very good mechanical properties and environmentally friendly manufacturing process. The development of basalt fiber technology is due to the need for materials resistant to high temperatures, non-flammable, non-corrosive, lightweight, and characterized by significant tensile strength (Sim, et al., 2005). Initially, basalt fibers were used as insulating material. This material proved to be an excellent substitute for asbestos fiber products in terms of insulation parameters and, at the same time, a material without carcinogenic properties. For these reasons, numerous research centres in the world are involved in the study of basalt as well as chopped and continuous basalt fibers, seeking new technologies for their production and use in the industry.

Basalt fibers are obtained from basalt rocks through melting and drawing process. Basalt ore are formed by the rock magma. During the rock magma forming process, associated with high temperature, high pressure and ambient pressure drop, the basalt ore is formed, which has extremely high chemical and thermal stability (Kabay, 2014, Wei et al., 2011). Therefore, the basalt fiber has inherited the basalt ore structure and performance characteristics, such as outstanding thermal stability, anti-corrosive performance, ideal heat insulation, sound absorption, and low moisture absorption. In addition, this fiber exhibits high strength and high module performance. The BFs do not need any other additives, which make additional advantage in cost (Wei et al., 2010). According to Sim et al. (2005) the BFs have better tensile strength than the E-glass fibers, greater failure strain than carbon fibers as well as good resistance to chemical attack, impact load and fire. These features, combined with lower cost, could make basalt fibers a suitable replacement for steel, glass, and carbon fibers in many applications (Borhan, 2012).

However, previous studies on the use of BFs in concrete are limited. Sim et al. (2005) investigated the properties of concrete containing continuous basalt fiber (produced from volcanic rock). The results show the improvement in thermal and mechanical properties of concrete. Limited research has studied the effect of short basalt fiber on mechanical properties of geopolymeric concrete (Dias et al., 2005, Li et al., 2009). Kabay (2014) reported that the addition of short basalt fibers resulted in decrease in compressive strength and at the same time the enhancement of fracture energy and reduction of abrasive wear of concrete. Branston et al. (2016) have determined that the fiber geometry (length and diameter) have a significant effect on the performance characteristics of concrete element under loading both in the pre-cracking and post-cracking range. However, the full potential of fiber reinforced concrete is still not fully exploited in practice (High et al., 2015, Sim et al., 2005).

Considering the applicability of basalt, fibers further experimental studies should be conducted on the use of BF in cement based composites to characterize its effects on physical and mechanical properties. Fracture mechanics is widely used to analyze the material behavior in a structure (Sim et al., 2005, Kabay, 2014, Wei et al., 2011). The relation between microstructure evolution and macroscopic response is crucial in the design and modelling of heterogeneous materials. Applications of fracture mechanics to concrete structures can provide a rational basis for both service performance and failure analysis and can lead to a better understanding of the design methods.

TABLE I
Properties of fibers used

Property	Basalt fibres
Fiber shape	straight
Length (mm)	50
Diameter (mm)	0.02
Tensile strength (MPa)	1680
Elastic modulus (GPa)	89
Denisty (kg/m^3)	2600

Therefore, the aim of the study was to evaluate the effect of basalt fibers content on the toughness and post-cracking behavior of concrete. The fracture characteristics for concretes with basalt fibers, such as critical stress intensity factor K_{Ic} and crack tip opening displacement $CTOD_c$ were assessed on beams with initial notches in three-point-bending test. The mechanical properties of concretes were determined as well.

II. Methodology

A. Materials and specimen preparation

Concrete mixtures were made with two cement types CEM I 42,5 R and CEM II/A-V 42,5 R. The cement content in all mixtures tested was 320 kg/m^3. The water to cement ratio was equal to 0,40 and 0,50. As an aggregate, the mixture of sand (fraction 0-2 mm) and a natural aggregate with a maximum diameter of up to 16 mm was used. The geometry and properties of basalt fibers were presented in Table 1. The basalt fibers were added to concrete at three contents (V_f) of 2,0; 4,0 and 8,0 kg/m^3, which gave volume fractions 0,075%; 0,15% and 0,31%, respectively. The fibers were added as a replacement of part of

coarse aggregate by volume. Comparatively, the properties of concretes with no added fiber were also tested.

The polycarboxylate polymer based super-plasticizer was used to minimize fiber clumping and enhance fiber dispersion in concrete mix (ACI 544, 1998). The super-plasticizer was applied in the amount of 1,0% of cement mass.

The dry aggregate was mixed with fibers followed by cement. The materials were dry mixed for 2 min before adding the water with super-plasticizer. Mixing continued for further 4 min. The time of mixing was considered sufficient for the proper dispersion of fibers in the mix without causing a "balling" effect. The specimens were vibrated in moulds and then stored under polyethylene cover for 24 hours.

For each fiber-dosage combination the notched beams of size 100×100×400 mm were prepared for fracture parameters determination. Every series was composed of four replicates Moreover, the beams (100×100×400 mm) for flexural strength were also cast and cubes (100×100×100 mm) for the compressive strength test were cut from them. After demoulding all specimens were cured in water at the temperature of 18±2ºC till they were tested.

B. Test methods

The flexural strength of concrete was defined by the load capacity at the first crack. The compressive strength was determined according to EN 12390-3 (2011) using cubes of size 100 mm.

The fracture performance of concretes with fibers and control concrete without reinforcement was tested in accordance with the recommendations of RILEM Fracture Mechanics Committee (1985, 1990). The notched beams of size 100×100×400 mm were used for three-point bending test corresponding to Mode I conditions. The initial saw-cut notch with a depth equal to 30 mm and width of 3 mm was located in the mid-span place. The geometry of specimen and the way of load were presented in Fig. 1. The elongated U-notches (a_0/d = 0,30) were sawn under wet conditions one day before the test. Each series was composed of 4 replicates.

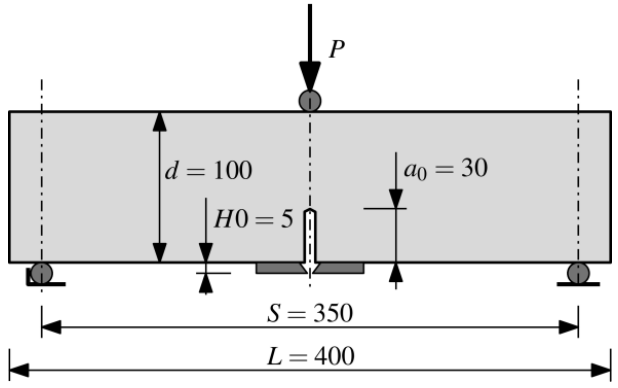

Fig. 1. Fracture testing configuration and geometry of notched specimen.

The universal testing machine (MTS 322) with closed-loop servo control was used to achieve a stable failure of specimens. The load-deflection (P-δ) curves and load – crack mouth opening displacement (P-CMOD) curves were determined for the fracture process analysis. At the same time the complete load-time curve was recorded to check the stability during the test. Fig. 2 shows the testing machine with beam specimen.

The clip gauge was used to measure the CMOD values. The length of gauge was chosen in such a way that possible errors caused by the bending effects were avoided. The rate of loading was controlled by the constant rate of increment of crack mouth opening displacement. The applied load was automatically reduced (unloading phase) when the load passed the maximum value and was about 95% of the peak load. When the applied load was reduced to 100 N, reloading was applied. The cycles of loading and unloading were repeated four times, and then the specimen was loaded up to failure.

Fig. 2. Notched beam specimen during testing.

The fracture parameters considered were the critical stress intensity factor K_{Ic} and the critical tip opening displacement $CTOD_c$. The critical stress intensity factor K_{Ic} is defined as the stress intensity factor calculated at the critical effective crack tip, using the measured maximum load. The critical crack tip opening displacement $CTOD_c$ is defined as the crack tip opening displacement calculated at the original notch tip of the specimen, using the measured maximum load and the critical effective crack length a_c. A crack of given length (a_0 = 30 mm in current analysis) critically propagate when it reaches the length of a_c. Based on K_{Ic} and $CTOD_c$ the critical effective crack length a_c was assessed. The parameters were determined using procedure and equations given in RILEM TC 89-FMT

Recommendation (1990), based on the fracture model (TPFM) elaborated by Jenq and Shah (1985), assuming cyclic loading-unloading test procedure. Both parameters are related to the critical stress σ_c initiating the crack propagation and the effective length of the critical crack a_c according to the following relationships:

$$K_{Ic}^{s} = \sigma_c \sqrt{\pi a_c}\, g_1\left(\frac{a_c}{b}\right) \quad (1)$$

$$\mathrm{CMOD}_c = \frac{4\sigma_c a_c}{E} g_2\left(\frac{a_c}{b}\right) \quad (2)$$

$$\mathrm{CTOD}_c = \mathrm{CMOD}_c g_3\left(\frac{a_c}{b}, \frac{a_0}{b}\right), \quad (3)$$

where g_1, g_2, and g_3 are geometrical functions.

The assessments for LEFM application by Jenq and Shah were described in details in Shah et al. (1995).

The fracture energy (G_F) is defined as the area under the load-deflection curve per unit fractured surface area. The fracture energy of concretes tested in this experimental study, was evaluated using the equation given by RILEM TC 50-FMT Recommendation (1985), in which energy was calculated from load-deflection curves obtained by performing a three-point bending test according to equation:

$$G_F = \left[\int_0^{\delta_{\max}} P(\delta)d\delta + mg\delta_{\max}\right] / \left[(d - a_0)b\right], \quad (4)$$

where g = 9,81 m/s^2; d – beam depth; b – beam width; a_0 – notch depth and δ_{max} – maximum deflection. In connection with the test, the weight of the beam m was determined and included into calculation of G_F.

The scatter of the calculated values of G_F results from the inevitable random length of the tail region of P-δ curve and also from the uncertainty in extrapolating the curve descent to zero. To reduce the impact of factors mentioned on the scatter of G_F the plot was cut down when the load was approximately equal to 0,05 P_{max} (100÷200 N). On this basis, the value of δ_{max} was determined. The area of the cross section of specimen, to which the total energy value was referred, was determined based on the width of the test specimen b and the depth d excluding the notch (a_0 = 30 mm).

III. Results

The test results of selected mechanical properties, determined after 28 days of curing, characterizing the concretes tested, were presented in Table 2. The increase in basalt fiber content caused slight increase in compressive strength and significant increase in flexural strength of concretes tested. The strength parameters were also determined by the type of cement used and the w/c ratio. Generally, better performances were obtained for concretes containing CEM I 42,5 R cement then CEM II/A-V 42,5 R.

TABLE II
Measured average values of concretes with various content of fiber V_F: compressive strength F_{CM} and flexural strength F_{CTM}

Cement	w/c	V_f (kg/m^3)	f_{cm} (MPa)	f_{ctm} (MPa)
CEM I 42,5 R	0,40	0,0	67,54±1,89	4,51±0,20
		2,0	65,73±5,54	5,48±0,69
		4,0	72,77±5,55	4,89±0,67
		8,0	75,63±2,44	5,62±0,50
	0,50	0,0	65,17±6,70	4,14±0,49
		2,0	66,26±1,83	4,18±0,30
		4,0	70,67±8,05	5,00±0,51
		8,0	72,50±1,79	5,28±0,28
CEM II/A-V 42,5 R	0,40	0,0	52,28±2,63	5,03±0,18
		2,0	55,78±3,87	5,10±0,35
		4,0	58,26±4,36	5,64±0,40
		8,0	60,19±1,12	5,89±0,59
	0,50	0,0	51,09±4,07	4,84±0,23
		2,0	54,52±2,75	4,65±0,31
		4,0	54,87±2,08	4,89±0,46
		8,0	58,88±4,47	5,55±0,30

The fracture toughness (K_{Ic}) and the critical crack tip opening displacement (CTOD_c) were determined on the basis of load P vs. CMOD curves obtained for the concrete specimens subjected to cyclic loading-unloading. The initial parts of characteristic P–CMOD plots obtained for concretes with w/c=0,40 made of CEM I 42,5 cement are shown in Fig. 3 and for concretes made of CEM II/AV 42,5 R cement - in Fig. 4.

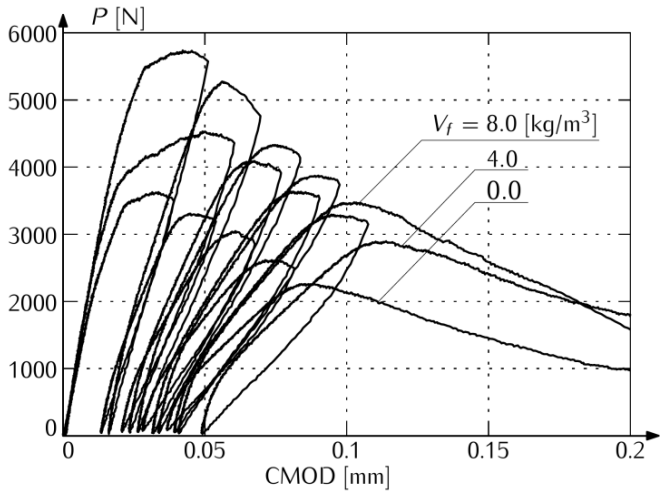

Fig. 3. Load P-CMOD plots for concretes with w/c = 0,40 (CEM I 42,5 R) with different content of basalt fibers V_f.

The analysis of the P–CMOD plots (Figs 3 and 4) showed

that as the fiber content increased, the length of the linear segment of the first phase of graph (elastic phase) increased. After the linear segment of *P*–CMOD curve, deviation from a linear response is observed and the load reaches the maximum value, which indicates the onset of the crack initiation at the tip of the notch. Increasing fiber content caused the increase in the value of critical load. In the stable pre-cracking phase, the *P*–CMOD relationship was nonlinear. When the maximum value of load was reached, the unstable crack development occurred. In the post-cracking range, the material softening and the gradual decrease in the load were observed with the increase of crack mouth opening.

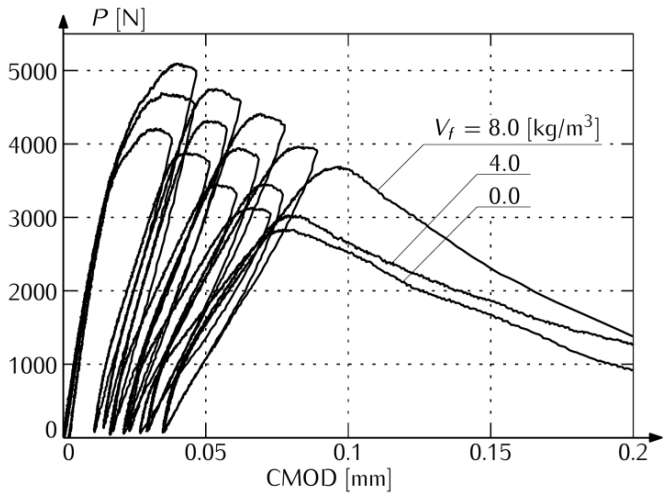

Fig. 4. Load P-CMOD plots for concretes with *w/c* = 0,40 (CEM II/A-V 42,5 R) with different content of basalt fibers V_f.

The results of the critical stress intensity factor (K_{Ic}) and the critical value of crack tip opening displacement $CTOD_c$, derived from the *P*–CMOD relationships for different fiber content, were shown in Figs 5 and 6, respectively. Comparing the mean values against the scattering the measurement results, it was found that the fiber content, type of cement and *w/c* ratio had significant influence on the values of both parameters.

The increase in fiber content resulted in a significant increase in K_{Ic}, which means an increase in fracture toughness. The greatest changes due to the incorporation of fibers were observed for concrete with CEM I cement. In comparison to control concrete without fiber, the composites of *w/c* ratio equal to 0,40 and 0,50, containing 4,0 kg/m^3 of fiber, achieved K_{Ic} values 26% and 38% greater, respectively. Further increasing the additive content to 8,0 kg/m^3 resulted in a K_{Ic} value increase not exceeding 10%. For concrete with *w/c*=0,40 and 0,50 made of CEM II cement, the addition of 4,0 kg/m^3 increased the critical stress intensive factor value by 25% and 15%, respectively.

It was found that increasing the fiber content up to 4.0 kg/m^3 resulted in an increase in $CTOD_c$. Greater differences in $CTOD_c$ values associated with basalt fiber reinforcement were observed for CEM I cement concretes.

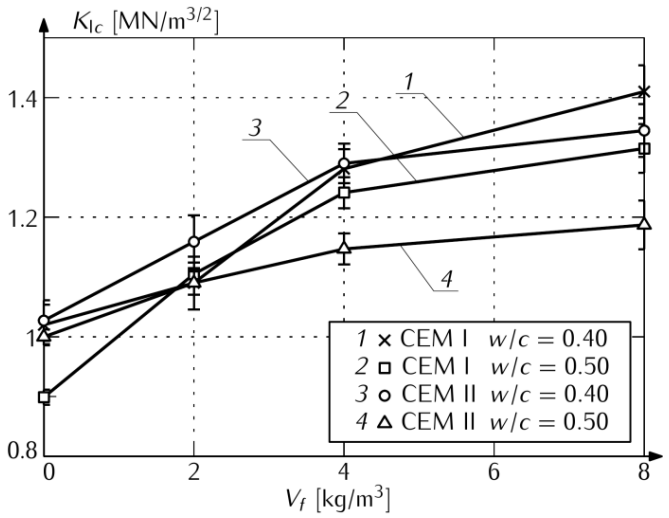

Fig. 5. Effect of fiber volume fraction V_f (%), cement type and *w/c* ratio on fracture toughness K_{Ic}.

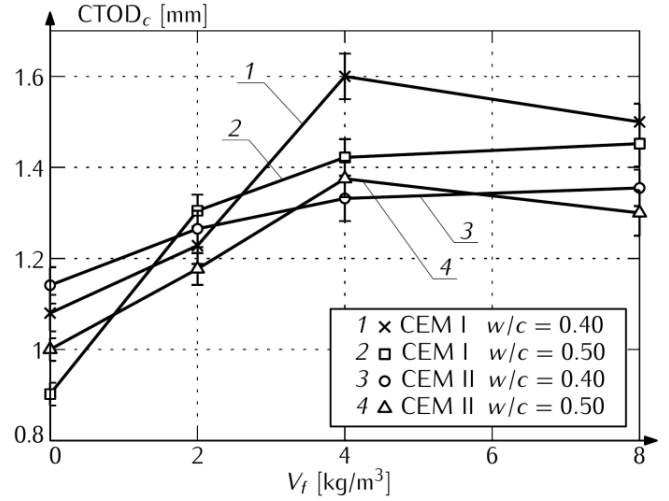

Fig. 6. Effect of fiber volume fraction V_f (%), cement type and *w/c* ratio on $CTOD_c$.

Until the crack is initiated, the load is transferred between the fibers and cement matrix by the adhesion forces and both the fibers and matrix are in an elastic state. As the load increases continuously, some of the microcracks may continue to develop until the deformation of the cement matrix reaches the limit value. Hence, *P*-CMOD plots show nonlinearity. Basalt fibers stretch across the micro-cracks performing a bridging effect by transferring stress and the test element is in a state of relative equilibrium. With further loading, the basalt fibers may break or be drawn from the cement matrix.

Fracture energy is characterizing the process of cracking and post-cracking strain softening of material after reaching the maximum stress. The dependence of fracture energy G_F on the fiber volume fraction, cement type and w/c ratio was shown in figure 7.

Growing fiber content has an increasing effect on the energy absorption. However, the significant effect of basalt fiber addition was observed for CEM I cement concretes. For CEM II cement concretes the increase in fiber content to 4,0 or to 8,0 kg/m^3 has very little influence on fracture energy. Probably, CEM I cement matrix is characterized by better bonding to basalt fibers.

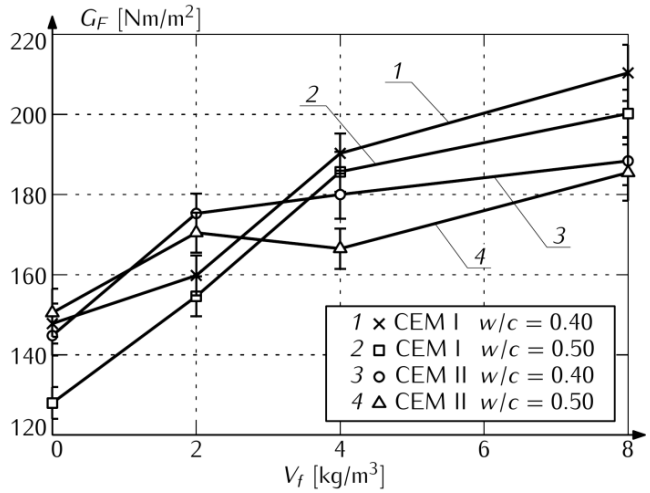

Fig. 7. Effect of fiber volume fraction V_f(%), cement type and *w/c* ratio on fracture energy G_F.

IV. Conclusions

The following conclusions can be drawn from the results presented in the paper. The results obtained may be useful in considering the practical applications of basalt fibers in concrete structural members.

1. The presence of chopped slender basalt fibres has no significant influence on compressive strength and flexural strength of concrete.
2. The analysis of the *P*-CMOD relationships show that dispersed reinforcement can significantly change the nature of the behavior of concrete members subjected to bending in both pre-cracking and post-cracking phases. The addition of basalt fiber in the tested amount of 2-8 kg/m^3 has improved the fracture mechanics parameters such as the critical stress intensity factor K_{Ic}, crack tip opening displacement CTOD$_c$, fracture energy G_F and recorded maximum values of load.
3. The changes in fracture mechanics parameters and the modification of *P*-CMOD plots, recorded under load, indicate that basalt fibers can increase the concrete resistance to initiation and propagation of cracks. It should be expected that the presence of fibers will change the brittle failure mode of concrete members to more ductile one.
4. The fracture parameters of concretes with basalt fibers are also determined by the type of cement. Better performances were obtained for concretes with CEM I 42,5 R then with CEM II/A-V 42,5 R.

Acknowledgment

This research work was financially supported by National Centre for Research and Development, Poland; project number PBS3/A2/20/2015 (ID 245084).

References

ACI 544. IR-96. State-of-the-art report on fiber reinforced concrete. Manual of concrete practice. Farmington Hills, 1998.

Borhan, T.M. (2012) Properties of glass concrete reinforced with short basalt fiber. Materials and Design, 42, 265-271.

Branston, J., Das, S., Kenno, S.Y., Taylor, C. (2016) Mechanical behavior of basalt fiber reinforced concrete, Construction and Building Materials, 124, pp. 878-886.

Dias, D., Thaumaturgo, C. (2005) Fracture toughness of geopolymeric concretes reinforced with basalt fibers. Cement & Concrete Composites, 27(1), pp. 49-54.

EN 12390-3. Testing Hardened Concrete: Compressive strength of test specimens, 2011.

High, C., Seliem, H.M., El-Safty, A., Rizkalla, S.H. (2015) Use of basalt fibers for concrete structures. Construction and Building Materials, 96, pp. 37-46.

Jenq, Y.S., Shah, S.P. (1985) Two parameter fracture model for concrete. Journal of Engineering Mechanics, 111, pp. 1227-1241.

Kabay, N. (2014) Abrasion resistance and fracture energy of concretes with basalt fiber. Construction and Building Materials, 50, pp. 95-101.

Li, W., Xu, J. (2009) Mechanical properties of basalt fiber reinforced geopolymeric concrete under impact loading, Material Science Engineering A, 505(1-2), pp. 178-186.

Recommendation TC 50-FMT RILEM (1985) Determination of the Fracture Energy of Mortars And Concretes By Means of Three-Point Bend Tests on Notched Beams. Materials and Structures, 18, pp. 285 – 290.

Recommendation TC 89-FMT RILEM (1990) Determination of fracture parameters (KIc and CTODc) of plain concrete using three-point bend test. Materials and Structures, 23, pp. 457-460.

Shah, S.P., Swartz, S.E., Ouyang, Ch. (1995) Fracture mechanics of concrete: Applications of fracture mechanics to concrete, rock and other quasi-brittle materials. John Wiley & Sons, New York,1995.

Sim, J., Park, C, Moon, D. (2005) Characteristics of basalt fiber as a strengthening material for concrete structures. Composites Part B: Engineering, 36, pp. 504-512.

Wei, B., Cao, H., Song, S. (2010) Environmental resistance and mechanical performance of basalt and glass fibers. Materials Science and Engineering A, 527, pp. 4708-4715.

Wei, B., Cao, H., Song, S. (2011) Surface modification and characterization of basalt fibers with hybrid sizings. Composites: Part A, 42, pp. 22-29.